Research Article

Giuseppe Lacidogna* and Federico Accornero

Elastic, plastic, fracture analysis of masonry arches: A multi-span bridge case study

https://doi.org/10.1515/cls-2018-0001
Received Nov 03, 2017; accepted Nov 10, 2017

Abstract: In this work a comparison is presented between elastic, plastic, and fracture analysis of the monumental arch bridge of Porta Napoli, Taranto (Italy). By means of a FEM model and applying the Mery's Method, the behavior of the curved structure under service loads is verified, while considering the Safe Theorem approach by Heyman, the ultimate carrying capacity of the structure is investigated. Moreover, by using Fracture Mechanics concepts, the damage process which takes place when the conditions assessed through linear elastic analysis are no longer valid, and before the set-in of the conditions established by means of the plastic limit analysis, is numerically analyzed. The study of these transitions returns an accurate and effective whole service life assessment of the Porta Napoli masonry arch bridge.

Keywords: Masonry arch bridge, Mery's Method, Limit analysis, Fracture mechanics, Structural stability, Architectural design

1 Introduction: Elastic, plastic, fracture analysis of masonry arches

Along the centuries, different critical approaches have been used to address the problem of masonry arch design methods [1–4]. Navier (1833) was the first to observe accurately the distribution of stresses at the interfaces between arch segments. To analyze the stress distribution over a cross-section, he introduced the thrust line concept, proving that the resulting line of action is to lie within the central kern in order to prevent tension. Mery's studies (1840) gained widespread recognition in the field of arch structures design. His method was based on the use of a graphic procedure in order to check the thrust line in agreement with the stress limitations identified by Navier [5]. Alberto Castigliano (1879) addressed the problems arised within the Theory of Elasticity by applying the minimum strain energy theorem to masonry arches [6], and introducing the concept of an *elastically imperfect system*. As a matter of fact, the concepts of homogeneity and isotropy were far from the real conditions of damaged and cracked materials.

The rigid blocks model used in the XVIII century to study masonry arches behaviour underwent major revisions during the last century, due to the various experiments carried out on arch models [1, 7–11]. One of the most significant revisions with respect to the eighteenth century theories was formulated by Heyman [8–10] and his school [11]. Referring back to Kooharian's studies [7], he applied the plastic limit analysis theorems to the issue of masonry arches stability, introducing three basic assumptions for such application: "stone has no tensile strength; stone has infinite compressive strength; the sliding of a stone on another cannot occur" [8].

Starting from these assumptions, the formation of a hinge is acknowledged right where the thrust line is tangent to the arch at the extremities. Three tangent points lead to the formation of three hinges: the limit to trigger a kinematic collapse mechanism lies in the formation of a fourth hinge. The limit analysis consists in the identification of the lowest possible load multiplier that generates a thrust line which is always contained within the arch volume and tangent to arch edges at four points (hinges).

Extensive studies have been recently carried out on arch and vaulted structures [12–18]. Several studies based on finite element analysis (FEM), and on non-linear FEM tension models [14, 17] show the potential of the method to compute both load-deflection curves and the interaction of the arch structure with the filling [12]. In particular, non-linear tensile behaviour models used in finite ele-

***Corresponding Author: Giuseppe Lacidogna:** Department of Structural, Geotechnical and Building Engineering - Politecnico di Torino (Italy); Email: giuseppe.lacidogna@polito.it
Federico Accornero: Department of Structural, Geotechnical and Building Engineering - Politecnico di Torino (Italy)

Figure 1: Taranto: Overview with Porta Napoli bridge location.

ment analysis arise directly from Fracture Mechanics theories [19].

Finally, other more recent methods [20–22] are proposed for the evaluation of masonry arch structures' stability, which consist in a evolutionary analysis of the fracturing process by means of Fracture Mechanics concepts.

This paper presents a comparison between elastic, plastic, and fracture analysis of the arch bridge of Porta Napoli, Taranto (Italy). The behavior of the bridge under service loads is verified by means of a FEM model and applying the Mery's Method. Moreover, considering the Safe Theorem approach by Heyman, the ultimate carrying capacity of the structure is also investigated. Finally, by using Fracture Mechanics concepts, the damage processes that take place when the conditions assessed through linear elastic analysis are no longer valid, and before the setin of the conditions established by means of the plastic limit analysis, are analyzed. The study of these gradual developments provides an accurate and effective whole service life assessment of the Porta Napoli masonry arch bridge.

2 The case study of the Porta Napoli bridge

The present analysis is devoted to the Porta Napoli masonry arch bridge. This structure is located in Puglia (Italy), in the city of Taranto, overlooking the natural channel at the northwest of the city, between the ancient town of Taranto and the new one (Figures 1, 2). The bridge was built starting from 1883, when a flood destroyed the bridge of 7 arcades constructed in the 10th century by the Byzantine rulers of Taranto.

The stone masonry structure has a total length of 130 m, and it consists of three shallow arches with a span of 14.3 m, and a rise of 2.4 m each (Figure 3). The bridge deck has a total width of 14 m.

The arch structure is composed by carparo stone blocks [23]. Carparo is a calcarenitic stone originated from limestone rock sediments, generally present in the marine environment. This particular limestone can be found in the coastal areas of Puglia, Italy. It presents a compression strength equal to 6.8 MPa, and a Young's modulus of 5.0 GPa. Like most of natural materials, carparo has no homogeneous appearance and may vary in grain size and color gradation depending on the concentration of its chemical components and on the different extraction points. During the centuries, carparo stone has been used as a building material as well as for decorative elements, fixtures and roofing.

Between the arch blocks of the Porta Napoli bridge, a lime mortar is interposed with the same mechanical characteristics of carparo stone [23].

The bridge of Porta Napoli is considered as a crucial part in the history of the city of Taranto, and over the centuries it has undergone profound changes [23, 24].

There is much uncertainty about the date of construction of the first bridge. The tradition gives the merit of its

Figure 2: Porta Napoli bridge. View from Mar Piccolo.

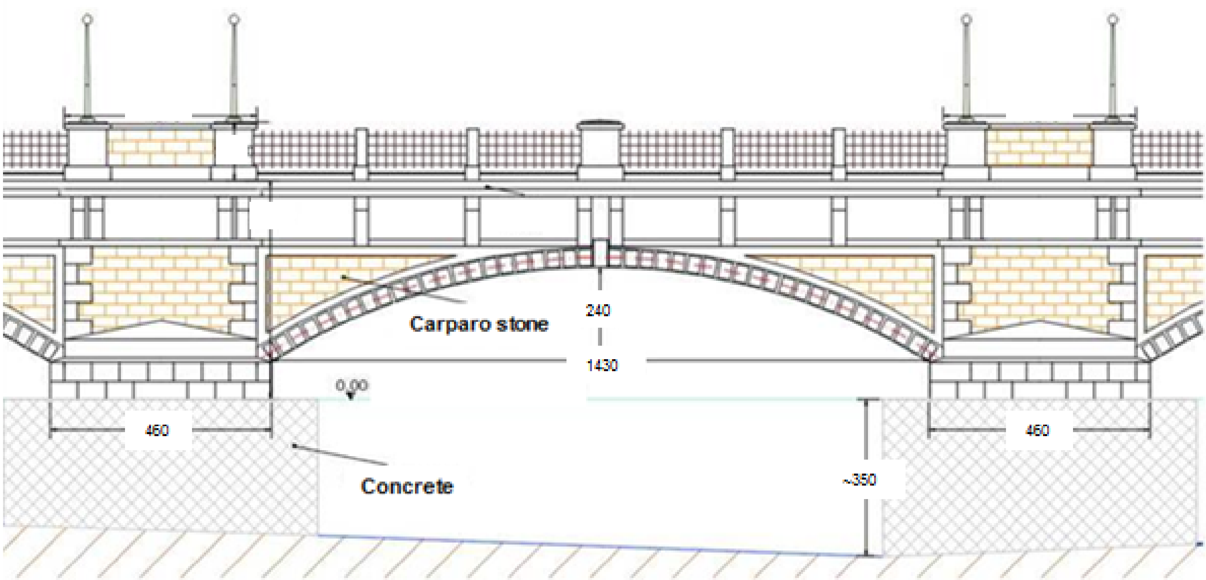

Figure 3: Porta Napoli arch scheme.

construction to the Byzantine Emperor Niceforo II Foca, around 987 a.C. As evidenced in [23, 24], in 1871 the bridge was 133 m long, 7 m wide, equipped with 7 arches, and two drawbridges, one overlooking the old town square, while the other in the center of the bridge itself, for the passage of large boats to the harbor. The night between September 14 and 15, 1883, an extreme cloudburst shook the whole city of Taranto. The flood caused the sea level rise, and the collapse of the millenary bridge. The current bridge was completed in 1906.

3 Finite Element and Mery's Method analyses

A 3D finite element model of the Porta Napoli bridge is performed using *Sap2000*® code, developed by Berkeley's CSI [25]. The FEM model consists of 10088 nodes and 8160 SOLID elements (Figure 4). These prismatic elements (Figure 5) allow to represent three-dimensional stress conditions. They are characterized by quadrangular and triangular faces, and they are generated by extrusion. Triangular elements are used between quadrangular prisms, in order to guarantee the structural continuity.

Table 1: Porta Napoli arch: Maximum compressive stresses following Mery's Method.

Section	0	1	2	3	4	5	6	7	8	9	10
Max compressive stress [MPa]	2.94	1.28	1.20	1.14	1.11	1.09	1.11	1.14	1.20	1.28	2.94

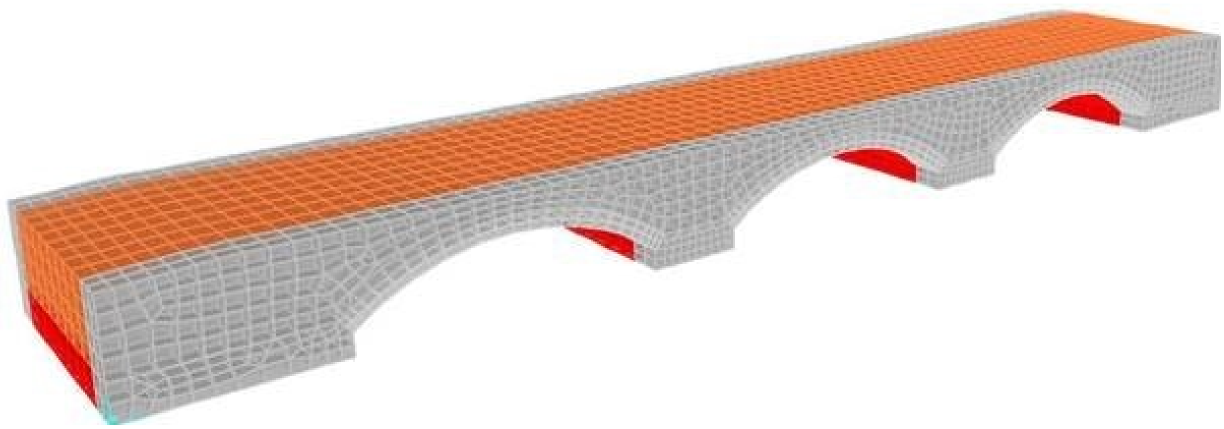

Figure 4: FEM model of Porta Napoli bridge

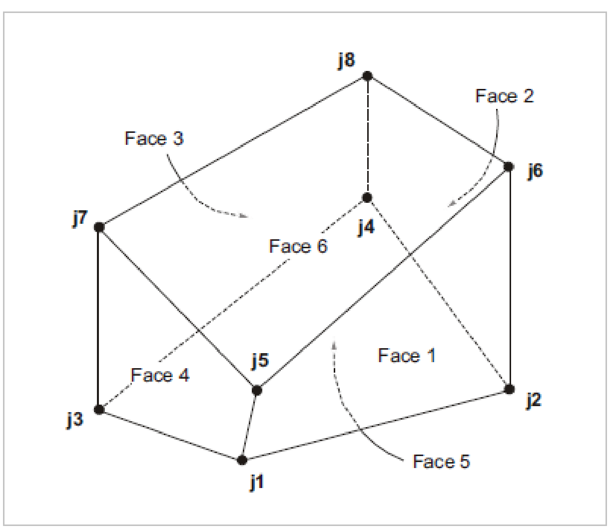

Figure 5: *Sap2000*®: Eight-node SOLID element.

In addition to the dead load representing the structural self weight, live loads are considered according to [26], and consisting in a uniformly distributed load equal to 9 kN/m^2, and two tandem loads of 300 kN each. Fixed ends are laid under abutments and piers of the Porta Napoli bridge.

In the following, the deformed shape of the Porta Napoli bridge (Figure 6) under service loads, and the principal stress contour (Figure 7) are shown. Note that the software *Sap2000* returns colors from blue (tension) to magenta (compression). In particular, it can be interesting to remark that the maximum vertical displacement of the bridge occurs in the key of arches, and it is equal to 5.1 mm; while the maximum compressive stress occurs at the arch springings, and it is about 3.5 MPa.

Moreover, applying Mery's Method and dividing the Porta Napoli single span arch in 10 blocks of unit width (Figures 8, 9), a maximum compressive stress occurs at the arch springings of about 3.0 MPa (see Table 1).

The thrust line calculated after Mery, remains within the arch thickness in the whole structure. In particular, except for the springings, this curve is contained within the middle third of the arch: it means that, under the action of service loads, the arch structure can be considered as safe, even if slight tension stresses occur at the imposts (Mery's hinges).

The results obtained within the elastic analysis indicate a trapezoidal pattern of the compression stress (Figure 9), with values that remain largely below the compressive strength of the carparo stone.

4 Plastic or Limit analysis

Considering the classic elastic analysis, some doubts may arise: *e.g.*, if one of the arch fixed supports is subjected to a slight displacement, this would be accompanied by a large variation in the thrust line configuration. In this condition, the "real" state of an arch structure is arbitrary: the shift, even imperceptible, of the arch configuration pro-

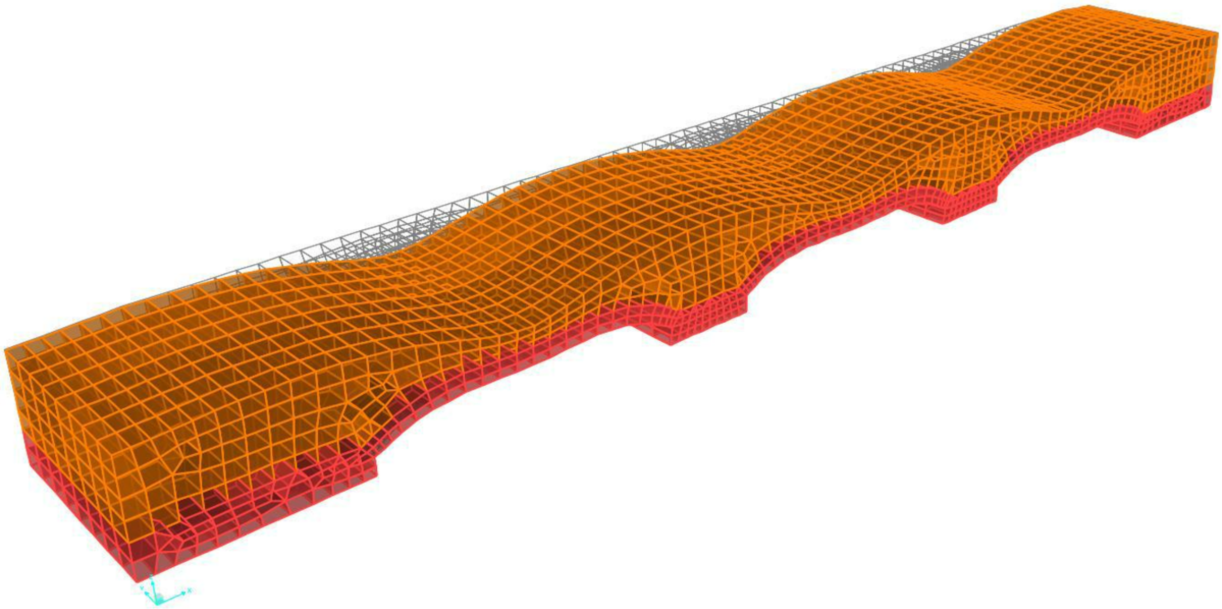

Figure 6: Porta Napoli bridge deformed shape.

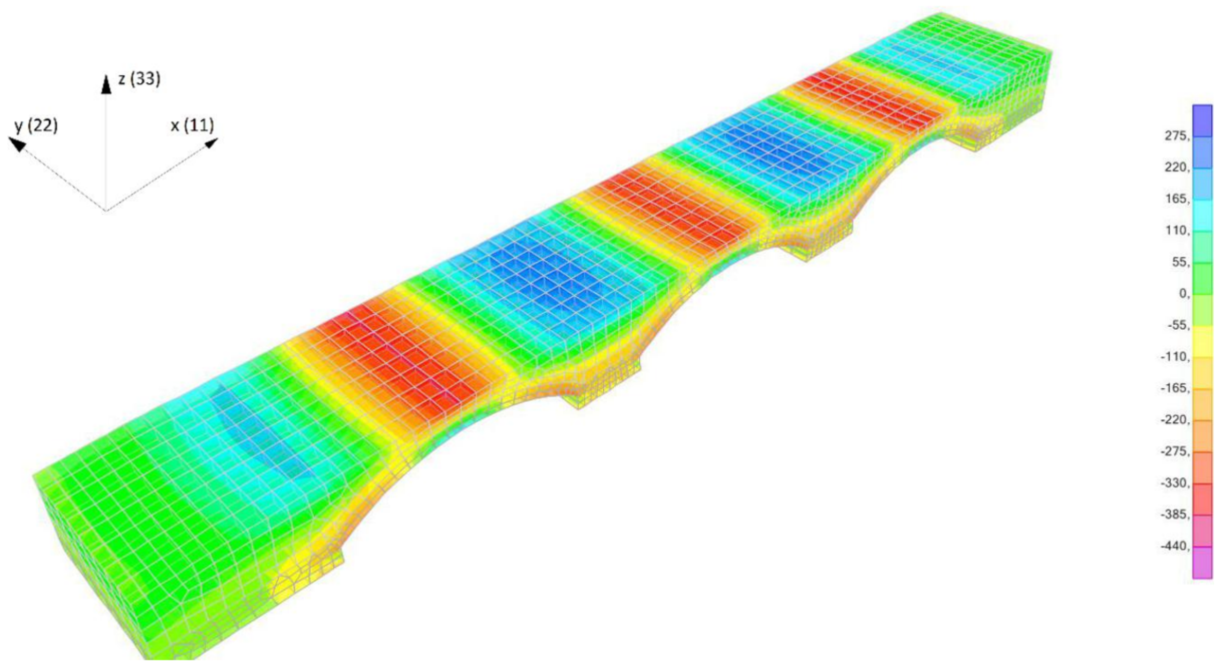

Figure 7: Porta Napoli bridge principal stress contour.

duces a state of equilibrium completely different from the original one. If the supports of an arch move, the arch itself will fit into a new state of equilibrium, almost forming three hinges. If the thrust line is contained within the arch thickness, the arch is then stable. This limit, following Heyman [8, 9], is represented by the collapse condition, which occurs, under perfect symmetry, at the formation of the fourth hinge.

Heyman's limit analysis sets the maximum strength offered by an arch structure, and looks for external actions for which the structure no longer can ensure the global equilibrium, and it is therefore destined to collapse by forming a mechanism.

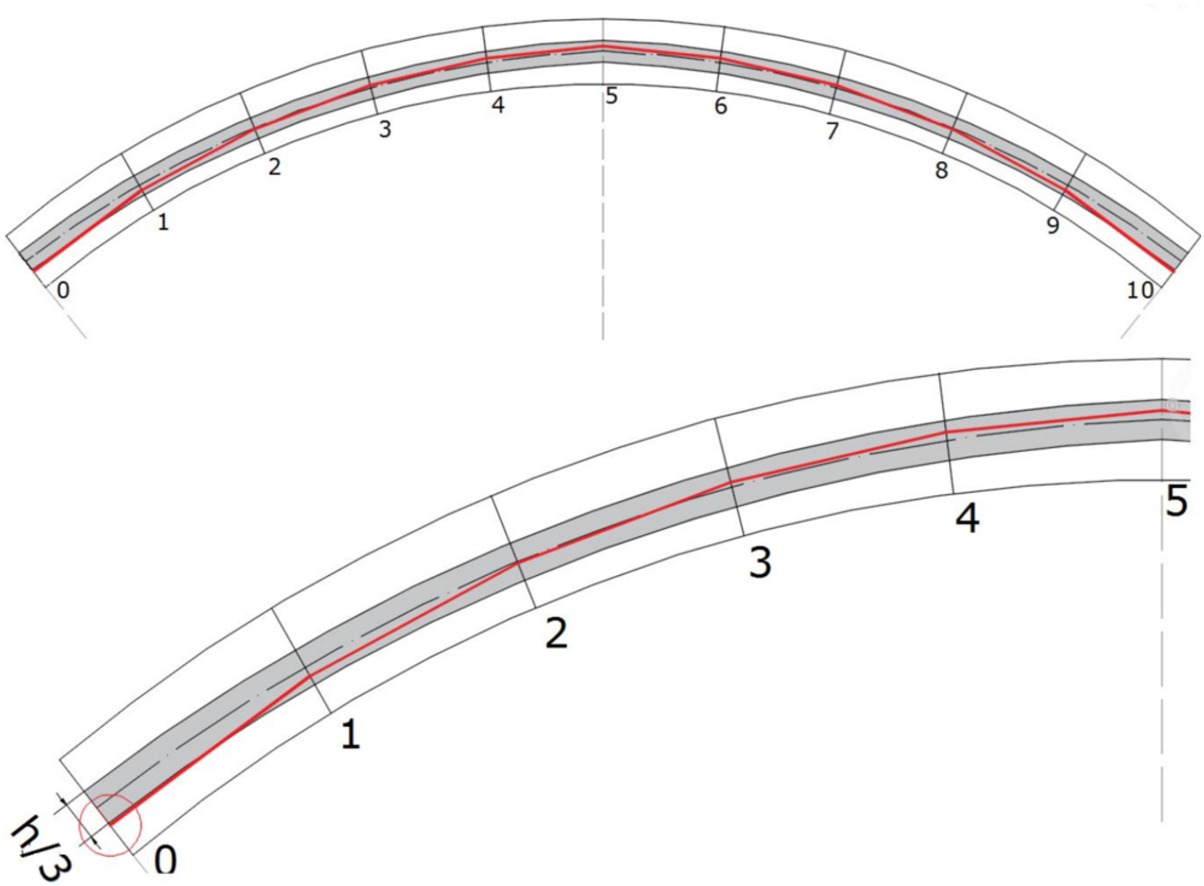

Figure 8: Thrust line of the Porta Napoli arch.

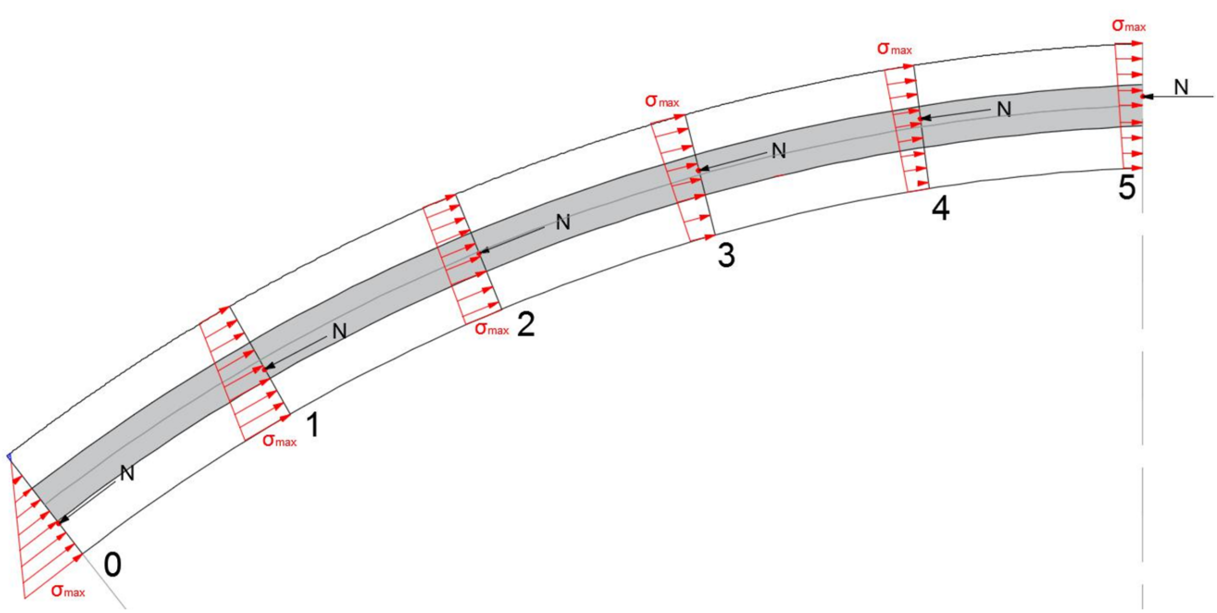

Figure 9: Thrust line of the Porta Napoli arch. Half of the structure.

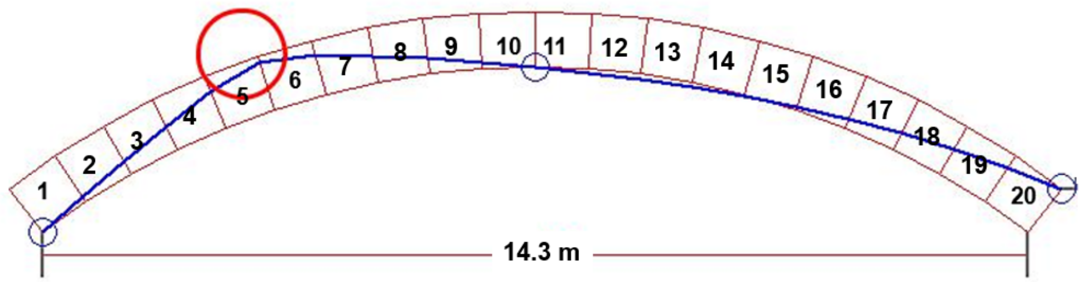

Figure 10: Thrust line of the Porta Napoli arch, after Heyman's Limit analysis.

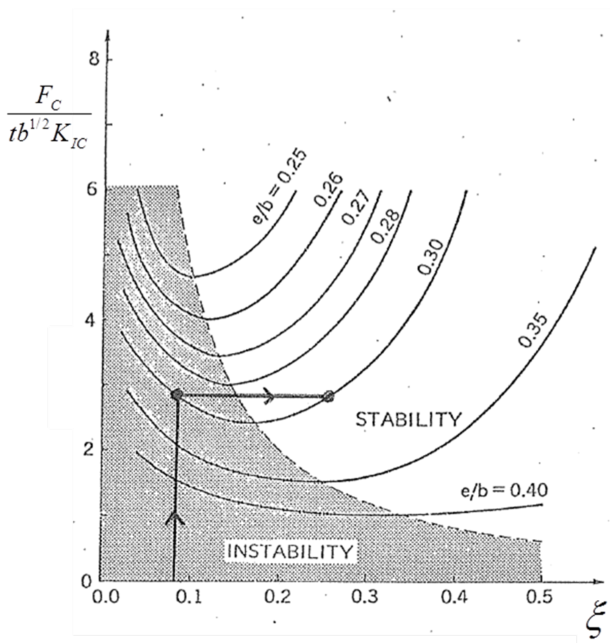

Figure 11: Fracturing process for off-center compression.

For the purpose of computing the Heyman limit load, the code *ARCO* (http://gelfi.unibs.it/arco.htm), developed by the University of Brescia (Italy) is used. This software is an analysis tool for masonry arches and vaults based on the Safe Theorem of the plastic analysis method [9].

Dividing the Porta Napoli arch structure in 20 blocks of unit width, and applying Heyman's method, it can be found that a maximum live load equal to 630 kN generates the onset of the fourth hinge between the fifth and the sixth block, and triggers the kinematic collapse of the structure, as can be seen in Figure 10.

This load results to be about 2 times larger than the maximum live load employed in the previous analyses for the same arch of unit width [26].

5 Fracture analysis

As previously stated, this method allows to capture the arch damaging process, which takes place when the conditions assessed through linear elastic analysis are no longer valid, and before the set-in of the conditions established by means of the plastic limit analysis. The evolutionary analysis of fracturing process numerically assesses how the arch structural behaviour is affected by cracks formation, as well as by the internal stress redistribution [20–22]. By this damage assessment, it can be clarified how the maximum admissible load evaluated by means of Linear Elastic Fracture Mechanics (LEFM) is larger than the load predicted by the Theory of Elasticity. Such an increase in terms of maximum admissible load can be defined "fracturing benefit", and it is analogous to the "plastic benefit" of the plastic limit analysis.

The analytical model representing the evolution of the fracturing process in masonry arches is fully described in [21, 22]. Setting both the structure's geometrical characteristics and the material's mechanical properties, in addition to the fracture toughness of the carparo stone (K_{IC} = 32.0 N/mm$^{3/2}$), the Porta Napoli arch is analysed through a FEM model in which the masonry structure is clamped to rigid abutments.

Such calculation adopts a step-by-step loading process. For each load increment, the code returns the related crack depth in the damaged section, which becomes a so-called brittle hinge [27]. In Figure 11, the brittle hinge behavior is described in terms of LEFM [21, 22], having the parameter ξ as the damage rate (crack depth to section height b), t as the section width, F_C as the axial force acting in the arch section, and e the eccentricity of F_C with respect to the section centroid. By increasing the load, the arch cross-section's inefficiency occurs when the crack depth is larger than the 70% of the arch section (fracturing collapse: ξ > 0.7). The same inefficiency takes place also when the compressive strength is reached (crushing failure).

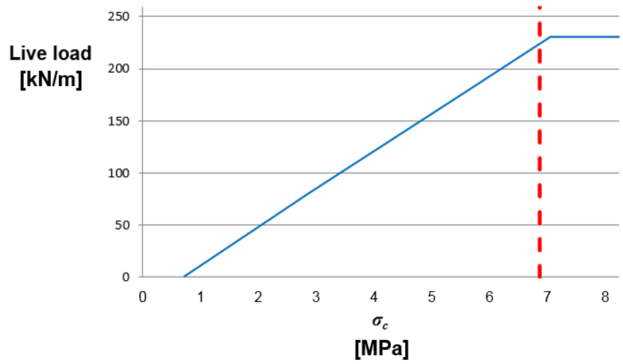

Figure 12: Porta Napoli bridge. Brittle hinges at the springings: Compressive stress vs live load.

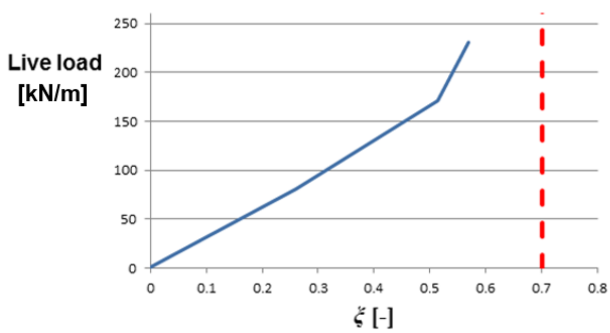

Figure 13: Porta Napoli bridge. Brittle hinges at the springings: Damage rate vs live load.

For the Porta Napoli arch, the fracture analysis code returns a uniformly distributed live load equal to 230 kN/m. At this point, a crushing failure at the springings takes place, and the structural scheme is modified by placing two hinges instead of the crushed sections. Figures 12 and 13 show the trend of the compressive stress and the damage rate ξ for the two brittle hinges at the springings. When the load reaches the value of 230 kN/m, the compressive stress acting in the ligament (Figure 12) exceeds the resistance offered by the carparo stone (crushing failure), while the damage rate of the arch section still remains under the limit of fracturing failure (Figure 13).

6 Conclusions

In this paper a comparison is presented between elastic, plastic, and fracture analysis of the monumental arch bridge of Porta Napoli, Taranto (Italy).

First, the behavior of the bridge under service loads, provided by the Italian national regulations on constructions, has been verified utilizing Theory of Elasticity concepts by a FEM linear model and applying the Mery's Method.

Then, the ultimate carrying capacity of the structure was investigated considering the Heyman's Safe Theorem approach.

Finally, the damage process which takes place by increasing the live loads and when the conditions assessed through linear elastic analysis are no longer valid, was numerically analyzed by using Fracture Mechanics concepts. This process, that takes into account the fracture initiation and propagation at the arch springings, occurs before the set-in of the conditions established by means of the plastic limit analysis.

The study of these transitions returns an accurate and effective whole service life assessment of the Porta Napoli masonry arch bridge, and more in general for a great number of similar historical masonry structures still having strategic importance in the infrastructure systems.

Acknowledgement: The authors are grateful to Eng. Luigi Palma for the collaboration in the analysis of the historical monument.

References

[1] Page, J. (1993). Masonry Arch Bridges, HMSO, London.
[2] Block, P., De Jong, M.J., Ochsendorf, J.A. (2006) As hangs the flexible line: Equilibrium of masonry arches. The Nexus Network Journal 8:9-19.
[3] Brencich, A., Morbiducci, R. (2007) Masonry Arches: Historical Rules and Modern Mechanics, International Journal of Architectural Heritage, 1:165-189.
[4] Karnowsky, I. (2012) Theory of Arched Structures, Springer.
[5] Mery E, (1840) Équilibre des voûtes en berceau. Annales des Ponts et Chaussées, 1:50-70.
[6] Castigliano, A. (1879). Théorie de l'Equilibre des Systèmes Elastiques et ses Applications, Del Negro, Turin.
[7] Kooharian, A. (1953). Limit analysis of voussoir (segmental) and concrete arches, Journal of the American Concrete Institute, 89:317-328.
[8] Heyman, J. (1966) The stone skeleton, International Journal of Solids and Structures, 2:255-296.
[9] Heyman, J. (1982). The Masonry Arch, Ellis Horwood, Chichester.
[10] Heyman, J. (1998) Structural Analysis: A Historical Approach, Cambridge University Press.
[11] Gilbert, M., Melbourne, C. (1994) Rigid block analysis of masonry structures, The Structural Engineering 72:356-361.
[12] Cavicchi, A., Gambarotta, L. (2007) Lower bound limit analysis of masonry bridges including arch-fill interaction, Engineering Structures, 29:3002-3014.
[13] Andreu, A., Gil, L., Roca, P. (2007) Computational analysis of masonry structures with a funicular model, Journal of Engineering Mechanics, 133:473-480.

[14] Betti M, Drosopoulos G.A, Stavroulakis G.E. (2008) Two non-linear finite element models developed for the assessment of failure of masonry arches. Comptes Rendus Mecanique 336:42-53.
[15] Proske, D., Gelder, P. (2009) Safety of historical stone arch bridges, Springer.
[16] De Arteaga, I., Morer, P. (2012) The effect of geometry on the structural capacity of masonry arch bridges, Construction and Building Materials, 34:97-106.
[17] Milani, G., Lourenco, P.B. (2012) 3D non-linear behavior of masonry arch bridges, Computer & Structures, 110:133-150.
[18] Moreira, V.N., Fernandes, J., Matos, J.C., Oliveira, D.V. (2016) Reliability-based assessment of existing masonry arch railway bridges, Construction and Building Materials, 115:544-554.
[19] Loo, Y.C., Yang, Y. (1991) Cracking and failure analysis of masonry arch bridges, Journal of Structural Engineering ASCE, 117:1641-1659.
[20] Carpinteri A., Carpinteri An. (1982) Softening and fracturing process in masonry arches. Proceedings of the 6th International Brick Masonry Conference, Rome 502-510.
[21] Carpinteri A, Lacidogna G, Accornero F. (2015) Evolution of fracturing process in masonry arches, Journal of Structural Engineering ASCE, 141:1-10.
[22] Accornero F, Lacidogna G, Carpinteri A. (2016) Evolutionary fracture analysis of masonry arches: Effects of shallowness ratio and size scale, Comptes Rendus Mécanique, 344:623-630.
[23] Belli, P. (2008) Ponti in Muratura di fine '800 nell'Italia Meridionale, Atti del Secondo Convegno Nazionale di Storia dell'Ingegneria, Cuzzolin.
[24] Risolvo, E. (2009) Strana Storia Tarantina, Scorpione Editrice.
[25] Brunetta, M., Bandini, L., De Lorenzi, M., Eds. (2006) SAP2000, Pordenone.
[26] Decreto del Ministero delle Infrastrutture 14 Gennaio 2008, Norme Tecniche per le Costruzioni, Gazzetta Ufficiale della Repubblica Italiana, 29, 4/2/2008.
[27] Taylor, N., Mallinder, P. (1993) The brittle hinge in masonry arch mechanisms, The Structural Engineer, 71:359-366.